

A Systems Approach for Improving Tea Aroma

Problem brought by
Charlie Hodgman¹, Alex Marshall¹, Jacquie de Silva²,

Report by
Jonathan Wattis³, Marcus Tindall⁴, Alan Champneys⁵ & Shyam Rallapalli⁶.

¹Multidisciplinary Centre for Integrative Biology, School of Biosciences,
University of Nottingham, Sutton Bonington, Leicestershire, LE12 5RD, UK.

²Unilever Research and Development, Colworth Science Park,
Sharnbrook, Bedford, MK44 1LQ, UK.

³Centre for Mathematical Medicine, School of Mathematical Sciences,
University of Nottingham, University Park, Nottingham NG7 2RD, UK.

⁴Centre for Mathematical Biology, Mathematical Institute,
24-29 St Giles, Oxford OX1 3LB, UK.

⁵Applied Nonlinear Mathematics Group, Department of Engineering Mathematics,
University of Bristol, Queen's Building, University Walk, Bristol BS8 1TR, UK.

⁶Sainsbury Laboratory, John Innes Centre,
Norwich Research Park, Norwich, NR4 7UH, Norfolk, UK

Charlie.Hodgman@nottingham.ac.uk alex@mycib.ac.uk Jacquie.De-Silva@unilever.com
Jonathan.Wattis@nottingham.ac.uk tindallm@maths.ox.ac.uk
A.R.Champneys@bris.ac.uk Ghanasyam.Rallapalli@bbsrc.ac.uk

Latest version: March 6, 2008

1 Introduction

The purpose of this report is to investigate the isoprenoid biosynthesis pathway which is relevant to the development of aromatic flavours in tea-production. The full pathway is complicated as demonstrated in the left panel of Figure 1. We shall focus on just one small part of the network which we believe to be an important factor in the production of nerolidol – one of the key products expressed in tea leaves.

In particular we investigate the metabolite concentration and gene expression levels during a twenty-hour timecourse in which the picked tea shoots undergo a variety of processes. These processes are detailed in the right-hand panel of Figure 1 and can be summarised as a series of withering and tumbling stages. During withering the leaves are left in a hot temperature environment; as well as drying out, this causes a stress response in the leaves which leads to a slow but extended production of chemicals and expression of certain genes. Withering stages generally last between 120 and 400 minutes. At three points during processing, the leaves are subjected to a short tumbling cycle

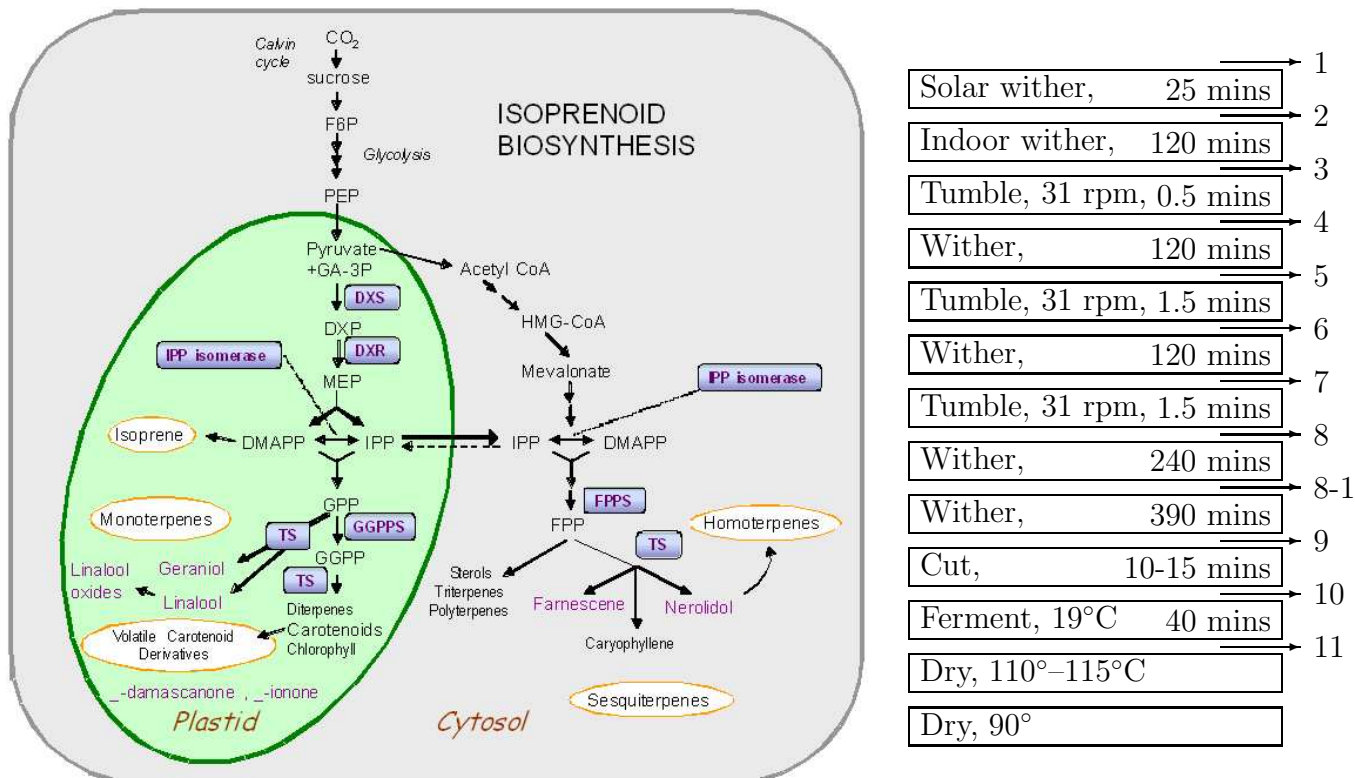


Figure 1: **Left:** Illustration of the genetic regulatory pathways. Inside the yellow ellipsoids are families of desired aromatic products, the purple boxed text indicates catalytic enzymes and the purple text denotes other desired aromatic products. **Right:** Table detailing the tea-making process giving the times of withering and tumbling.

(lasting between 30 and 90 seconds) in a drum rotating at 31 rpm. This causes wounding of the leaves which gives a similar but acute stress response. It also mixes the leaves and causes expressed aromatic species to be taken up by surrounding leaves. This part of the process is believed to stimulate the production of further aromatics.

1.1 Data analysis

We have analysed time-series data, provided by Unilever Research and Development, regarding the expression of key metabolites and genes during the course of the tea-making process. In this report we are concerned with differences between two different species, in both cases we consider the normal (wild type) case; no differences in expression due to mutations are considered.

The upper panels of Figure 2 show the levels of metabolite expression as functions of time for the two tea varieties of *Assamica* and *Sinensis* during the approximate 1000 minutes of the tea-making process. Whilst both show similarly high levels of Linalool, the significant curve we wish to focus on is that of E-nerolidol. This remains low during the processing of *Assamica*, but shows a marked increase at the end of the tea-making process in the case of *Sinensis*.

The lower panel of Figure 2 shows levels of gene expression throughout the tea-making process. Note the different scales: in the case of *Assamica* the vertical axis stops at six whilst that of *Sinensis* extends to 50. In *Assamica* all gene expression levels remain below five for all time; similar results

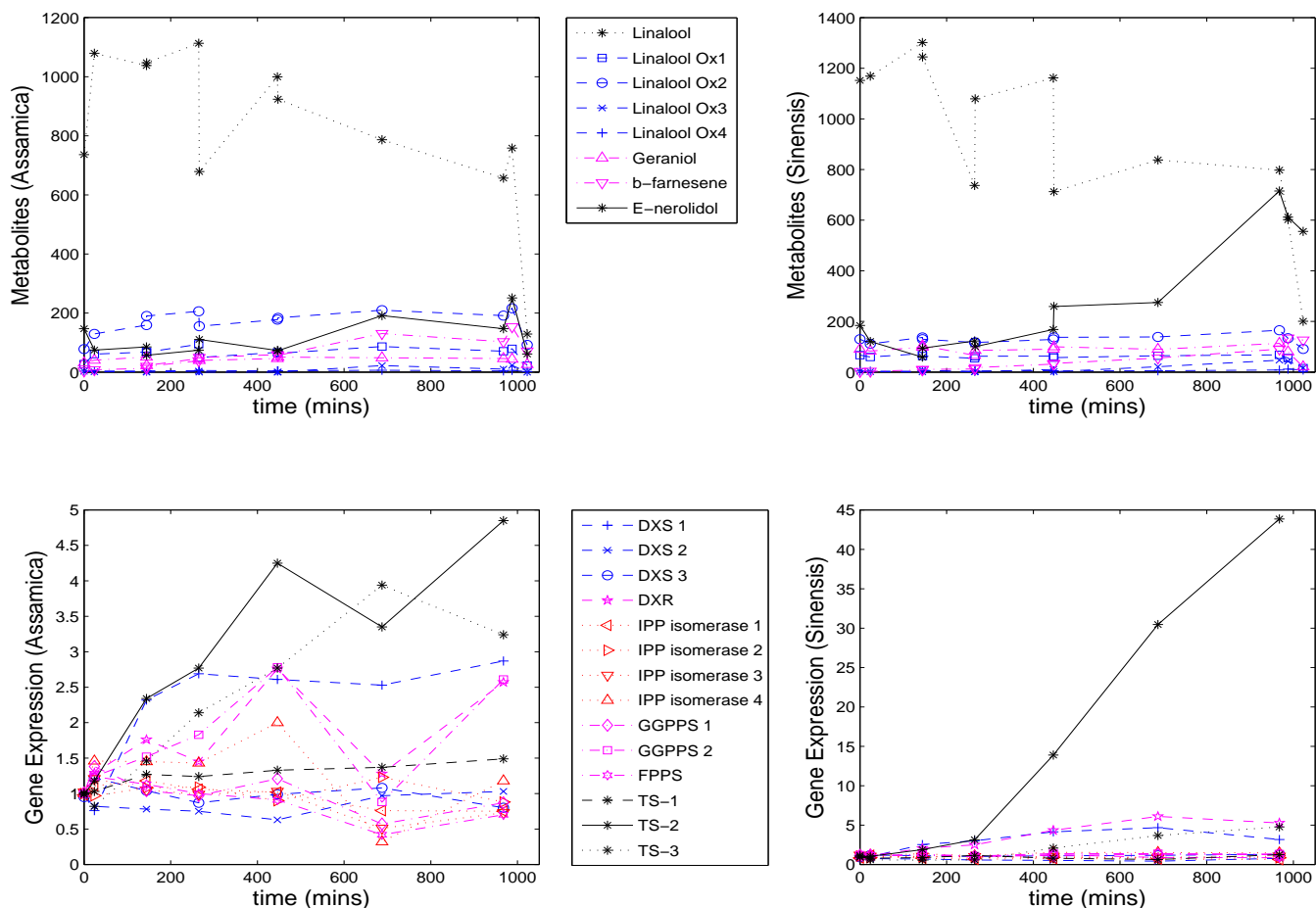


Figure 2: **Top left:** expression of metabolites plotted against time for the tea variety *Assamica*; **Top right:** expression of metabolites plotted against time for the tea variety *Sinensis*; **Lower left:** gene expression data plotted against time for the tea variety *Assamica*; **Lower right:** gene expression data plotted against time for the tea variety *Sinensis*.

are seen in *Sinensis* with the notable exception of terpene synthase, which we denote by *TS-2*, this gene is expressed at a significantly higher level.

The rise in the expression of *TS-2* and nerolidol is isolated from the other genes and metabolites in Figure 3. The top panel shows that in *Sinensis* (solid magenta trace) nerolidol abruptly rises after the first and third tumbles, at times $t \sim 150$ minutes and $t \sim 450$ minutes, with a significant rise overall from the start to the end of the tea-making process. During this time the level of nerolidol in *Assamica* (dashed blue trace) is approximately constant over the whole process. The lower panel of Figure 3 shows that the level of expression of *TS-2* rises in both *Assamica* and *Sinensis*; however, the rise of about four-fold in *Assamica* is dwarfed by the forty-fold increase in *Sinensis*.

The observed correlation between changes in *TS-2* expression and nerolidol concentration leads us to consider a simplified part of the isoprenoid biosynthesis pathway, specifically the lower right-hand-arm of the network diagram of Figure 1. Since the plastid is an organelle, it is encapsulated by a membrane inside the cell, hence we believe that the dominant aromatic compound is one expressed in the cytosol, namely nerolidol. Other, similar aromatic compounds are expressed inside the

plastid, but are less likely to become exposed to the atmosphere due to the membrane. In contrast, nerolidol is produced in the cytosol and thus easily released by withering and tumbling. Nerolidol is produced from the precursor metabolite FPP by the action of an enzyme, whose production is regulated by the gene *TS-2*. Hence it is the part of the pathway



It is the evolution of this part of the isoprenoid biosynthesis pathway that our models outlined in the next section will aim to explain. The network and equation (1) show that FPP is an important precursor for *TS-2*, so our models will also include a description of this.

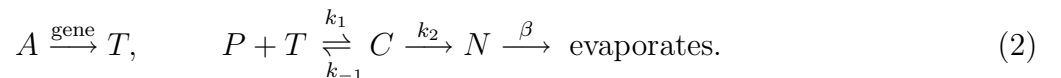
2 Mathematical modelling

We simplify the genetic pathway by introducing a single activator, A , which is produced in response to stress, caused by either withering or tumbling, and activates the gene *TS-2* to upregulate the production of its controlling enzyme T . We model the stress response in two ways: firstly, the long-time response due to withering, which occurs over several hours, and results in the constant production of A during the first part of the process; and secondly, the acute response to tumbling, which we model as a sudden sharp increase in the activator A . The activator species is allowed to decay throughout the process, and only when it is above a critical concentration do we assume it upregulates a gene which promotes the production of the enzyme T . The mathematical modelling of enzyme kinetic reactions is covered in many texts, such as Murray [3], Scott [4], more recently the modelling of the genetic regulation networks has been developed, for an introduction, see Alon [1].

2.1 Model 1

We assume that the whole of the withering process causes a constant production of both FPP which is denoted by P and T – the enzyme produced by the gene *TS-2*. We assume the enzyme is produced by the gene according to a activator-promoter mechanism (as opposed to an inhibitor-suppressor). Here, P and T are assumed to combine reversibly in a typical Michaelis-Menten reaction to form an intermediate complex denoted by $C = [P.T]$ which can decay to form the product nerolidol, denoted N . It is noted that other other chemical species are produced during this reaction, but these are ignored in the models presented here. Being aromatic, we assume that N is lost by evaporation at a rate proportional to its concentration.

Chemically, these mechanisms can be written as



Here k_1 is the rate at which P and T react, k_{-1} is the respective reverse reaction rate and k_2 is the rate of breakdown of C to form N which subsequently evaporates at a rate β . By applying the law

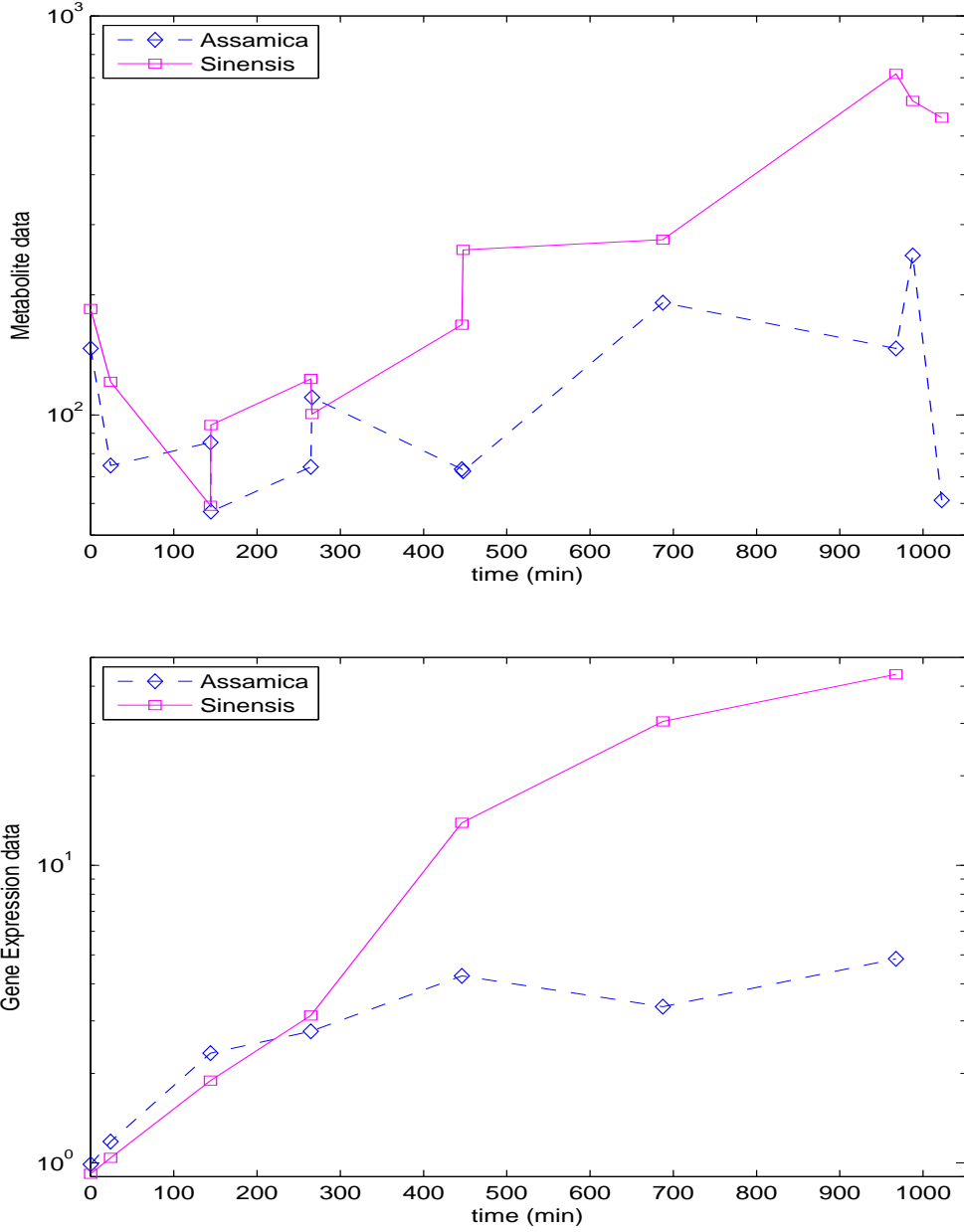


Figure 3: **Upper:** plot of nerolidol level against time, note the logarithmic scale on the vertical axis, and the step increases in the solid magenta curve (*Sinensis*) at $t \sim 150, 250, 450$ minutes, which correspond to the tumbling times. The blue dashed curve corresponds to data for *Assamica*. **Lower:** plot of *TS-2* expression level against time, again on a logarithmic scale, with magenta solid line for *Sinensis* data and blue dashed line for *Assamica*. Initially similar, the divergence starts following the second tumble at $t \sim 250$ minutes.

of mass action, we arrive at

$$\underbrace{\frac{dA}{dt}}_{\text{rate of change of activator conc.}} = \underbrace{k_5 H(\tau - t)}_{\text{increase in } A \text{ due to withering}} - \underbrace{\lambda A}_{\text{decay of activator}} + \underbrace{\sum_{j=1}^3 \gamma_j \delta(t - t_j)}_{\text{production of } A \text{ due to tumbling}} , \quad (3)$$

$$\underbrace{\frac{dP}{dt}}_{\text{rate of change of FPP conc.}} = \underbrace{k_{-1}C}_{\text{dissociation of } C} - \underbrace{k_1PT}_{\text{loss of } P \text{ to make } C} + \underbrace{\alpha_P}_{\text{constant production of } P}, \quad (4)$$

$$\underbrace{\frac{dT}{dt}}_{\text{rate of change of enzyme conc.}} = \underbrace{k_{-1}C}_{\text{dissociation of } C} - \underbrace{k_1PT}_{\text{loss of } T \text{ to make } C} + \underbrace{\alpha_T}_{\text{constant production of } T} + \underbrace{\frac{k_4A^q}{K^q + A^q}}_{\text{upregulated } T\text{-production by gene}}, \quad (5)$$

$$\underbrace{\frac{dC}{dt}}_{\text{rate of change of complex, } C} = \underbrace{k_1PT}_{\text{complex-(}C\text{)-formation}} - \underbrace{k_{-1}C}_{\text{dissociation of } C} - \underbrace{k_2C}_{\text{decay of } C \text{ to nerolidol}}, \quad (6)$$

$$\underbrace{\frac{dN}{dt}}_{\text{rate of change of Nerolidol conc}} = \underbrace{k_2C}_{N\text{-production from complex}} - \underbrace{\beta N}_{\text{evaporation of nerolidol}}. \quad (7)$$

We assume that P and T are produced at constant rates of α_P and α_T respectively, whilst A degrades at a rate λ . We assume that tumbling causes a further release of the T -precursor chemical A , where t_j are the times at which tumbling occurs and γ_j indicates the intensity of the tumbling process. Here, $H(\cdot)$ is the Heaviside function defined by

$$H(z) = \begin{cases} 1 & \text{if } z > 0, \\ 0 & \text{if } z < 0, \end{cases} \quad (8)$$

and $\delta(z)$ represents the Dirac-delta function modelling inputs at each of the tumbling times t_j . (This is defined by a spike of large amplitude situated at $z = 0$ such that $\delta(z) = 0$ for all $z \neq 0$ ($\delta(0) \neq 0$) yet has the property that $\int \delta(z) dz = 1$.) The k_4 term in equation (5) is due to the high level of A , namely $A > K$ causing the gene $TS-2$ to further up-regulate the production of T . This is modelled by a Hill function, where q is the Hill coefficient. This assumes that the gene $TS-2$ is responsible both for the background constant production of the enzyme T at a rate α_T and the increased rate when $A > K$. It is possible that these two production terms are caused by different genes, or that one is due to a different mechanism altogether.

The system of equations (3)–(7) is closed and subject to the initial conditions

$$A = A_0, \quad P = P_0, \quad T = T_0, \quad C = 0 \quad \text{and} \quad N = N_0 \quad \text{at} \quad t = 0. \quad (9)$$

The initial condition for N assumes there is an initial non-zero concentration of nerolidol already in the cell as a result of the natural metabolite processes shown in the left panel of Figure 1.

In the absence of tumbling ($\gamma_j = 0 \quad \forall j$) equation (3) decouples and can be solved to give

$$A(t) = \begin{cases} \frac{k_5}{\lambda}(1 - e^{-\lambda t}), & (t < \tau), \\ \frac{k_5}{\lambda}(1 - e^{-\lambda \tau})e^{-\lambda(t-\tau)}, & (t > \tau). \end{cases} \quad (10)$$

This solution is plotted in Figure 4, whose shape can also be seen in the lower curves in the left panels of Figures 5 and 6. The inclusion of tumbling modifies this curve into that seen in the

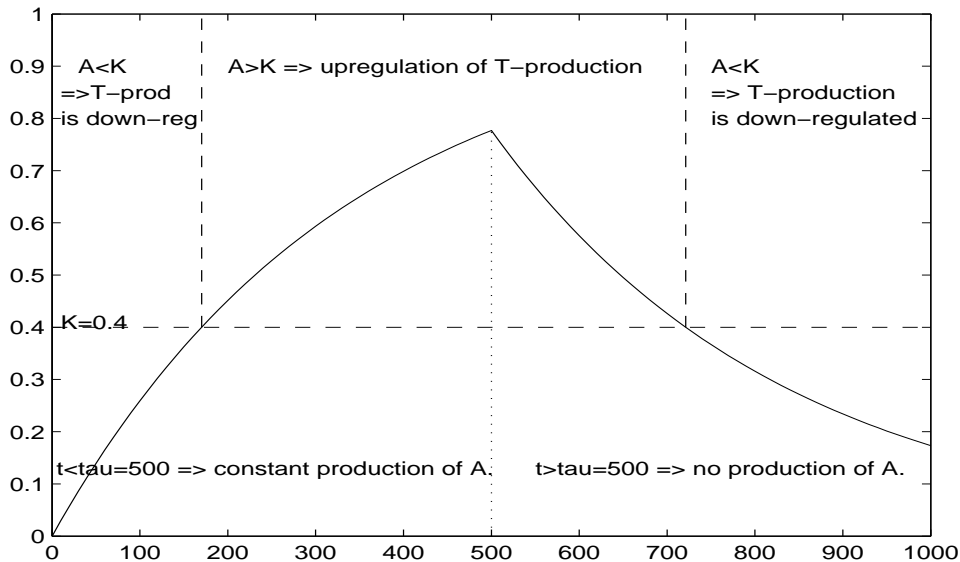


Figure 4: Evolution of the activator species A over time, for the case with no tumbling. We have also marked on the concentration $A = K$ where the level of A is large enough to cause the gene $TS-2$ to upregulate the production of the enzyme T , through the last term in equation (5).

right-hand panels of Figures 5 and 6, where A can be seen to be discontinuous across the tumbling events, due to sudden jumps at the times where tumbling occurs.

2.1.1 Parameter values

Little or no experimental data is available on the respective reaction rates in our model. We have, however, obtained error bounds on certain model parameters by undertaking a fit-by-eye of the model to the withering only response in the case of *Assamica*. These values are listed in Table 1. Estimates on parameters affecting the tumbling response have then been made using a further fit-by-eye.

We have assumed that the Michaelis-Menten reaction step is heavily biased in the forward directions, that is $k_2 \gg k_{-1}$, this implies that the process can simply be replaced by $P + T \rightarrow N$. However, the cases $k_{-1} \sim k_2$ and $k_{-1} \gg k_2$ could also be considered. This would lead to slower dynamics, where the complex (C) was more likely to dissociate into its reagents (P and T) than form the product N .

2.2 Model 1 Results

Solving the system of ordinary differential equations (3)–(9) in Matlab using Gear’s Method (ode15s) we find that the model demonstrates the correct behaviour in the change in nerolidol and enzyme (T) concentration for the wither only response as shown in the left panel of Figure 5. When tumbling is introduced as shown in the right panel of Figure 5, an increase in the enzyme

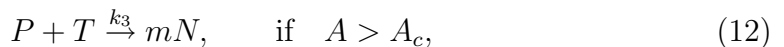
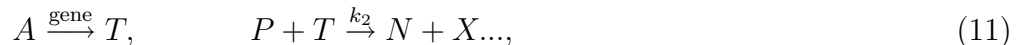
Parameter	Description	Value	Dimensions
k_1	Rate of formation of [P.T] complex.	1/60	M/min
k_{-1}	Reverse rate of [P.T] complex formation.	$1/60 \times 10^{-3}$	/min
k_2	Rate of nerolidol formation.	1/60	/min
k_4	Rate of enzyme T formation by activator (A).	1/21	M/min
k_5	Rate of activator production.	3×10^{-3}	M/min
K	Switching concentration of activator (A) for enzyme production (T)	0.4	M
q	Hill coefficient.	1	dimensionless
α_T	Rate of enzyme production (T).	0.04	M/min
α_P	Rate of FPP production.	0.02	M/min
β	Rate of nerolidol evaporation.	0.03	/min
λ	Rate of activator (A) degradation.	3×10^{-3}	/min
τ	Activator production time.	500	min
γ_j ($j = 1, 2, 3$)	Magnitude of activator (A) response to stress of j^{th} tumble.	2.0, 3.0, 3.0	M/min
t_j ($j = 1, 2, 3$)	Tumbling times.	144, 265, 446	min
P_0	Initial FPP concentration.	1.0	M
T_0	Initial enzyme concentration (T).	1.0	M
N_0	Initial nerolidol concentration.	1.4	M

Table 1: Parameter values.

activity is predicted, but this does not lead to an increase in nerolidol concentration as observed in the experimental data. In short, the up-regulation mechanism of nerolidol by the enzyme T is not large enough to cause an increase in nerolidol following an increase in T , as presented in the experimental data of Figure 3. This issue was not resolved by increasing the magnitude of each tumble ($\gamma_j = 0, \forall j$). We thus revise our model in the following section to account for this discrepancy.

2.3 Model 2 - Up-regulating nerolidol *via* the enzyme T

Our revised model seeks to ensure that enzymatic up-regulation leads to an appropriate increase in nerolidol concentration. To overcome this problem we revise our reactions as follows



where m is the number of additional nerolidol molecules created when the activator A is above the critical value (A_c) for further upregulation of the gene to occur. Here we have simply included an extra pathway by which nerolidol-production (N) is further up-regulated due to the presence of P and T . We note that A_c is a critical activator concentration whereby the second pathway up-regulating N by T is activated.

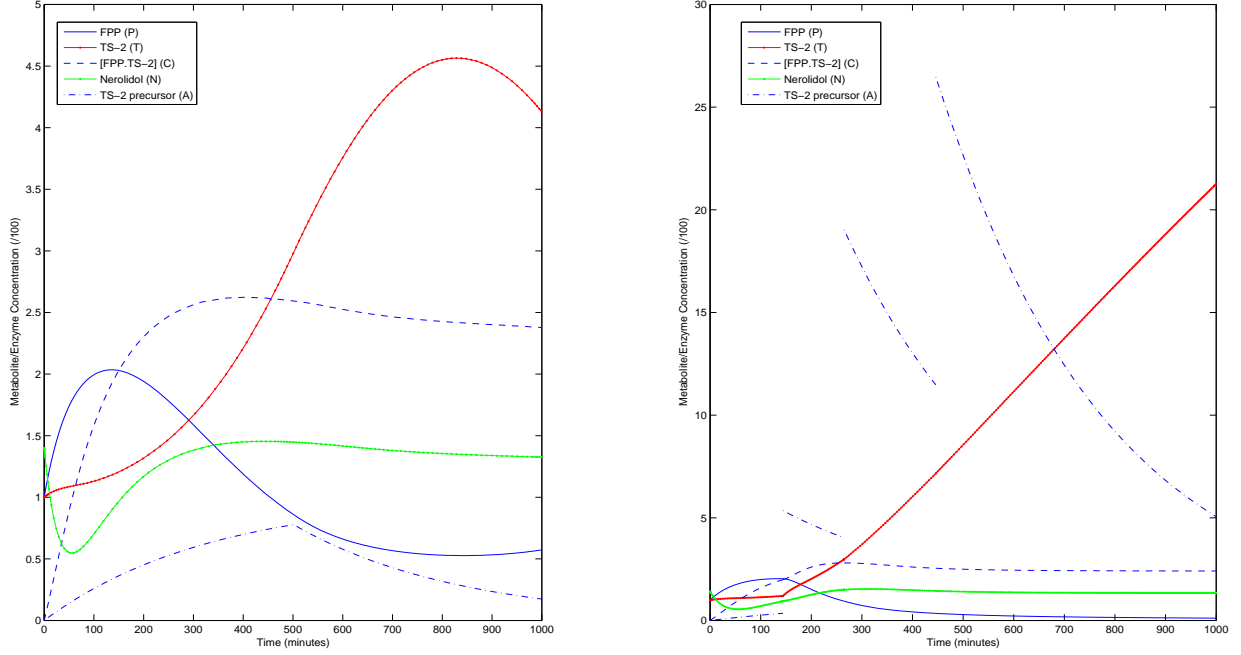


Figure 5: The predicted change in nerolidol concentration and enzyme (T) concentration for Model 1. The enzyme T is produced by the gene $TS-2$ so is used as an indicator of $TS-2$ gene expression. The **left** figure is for withering only (i.e. *Assamica*) whilst the **right** figure includes both withering and tumbling (i.e. *Sinensis*). Note the difference in enzyme concentrations between the two cases, but the limited or no change in nerolidol concentrations.

Applying the law of mass-action to equations (11) and (12) leads to

$$\frac{dA}{dt} = k_5 H(\tau - t) - \lambda A + \sum_{j=1}^3 \gamma_j \delta(t - t_j), \quad (13)$$

$$\frac{dP}{dt} = \alpha_P - k_2 PT - k_3(A)PT, \quad (14)$$

$$\frac{dT}{dt} = \alpha_T - k_2 PT - k_3(A)PT + \frac{k_4 A^q}{K^q + A^q}, \quad (15)$$

$$\frac{dN}{dt} = k_2 PT + m k_3(A)PT - \beta N, \quad (16)$$

where the respective initial conditions are given by equation (9). Here all rates are as previously defined for Model 1 with

$$k_3(A) = k_3 H(A - A_c). \quad (17)$$

Solving this system of equations using the previous parameter values detailed in Table 1 with the exception of

$$A_c = 1.5, \quad k_3 = k_2 = 1/60, \quad m = 4, \quad \gamma_1 = 5, \quad \gamma_2 = 15, \quad \gamma_3 = 15, \quad (18)$$

leads to the results shown in Figure 6. Here we note that the withering response of both nerolidol and the enzyme T is the same as that previously predicted (left-panel of figure), but increases in

both the enzyme T and the nerolidol concentrations are observed when tumbling is applied (right-panel of figure). Thus our model reproduces the qualitative and to a large degree, the quantitative behaviour observed in the experimental data of Figures 2 and 3.

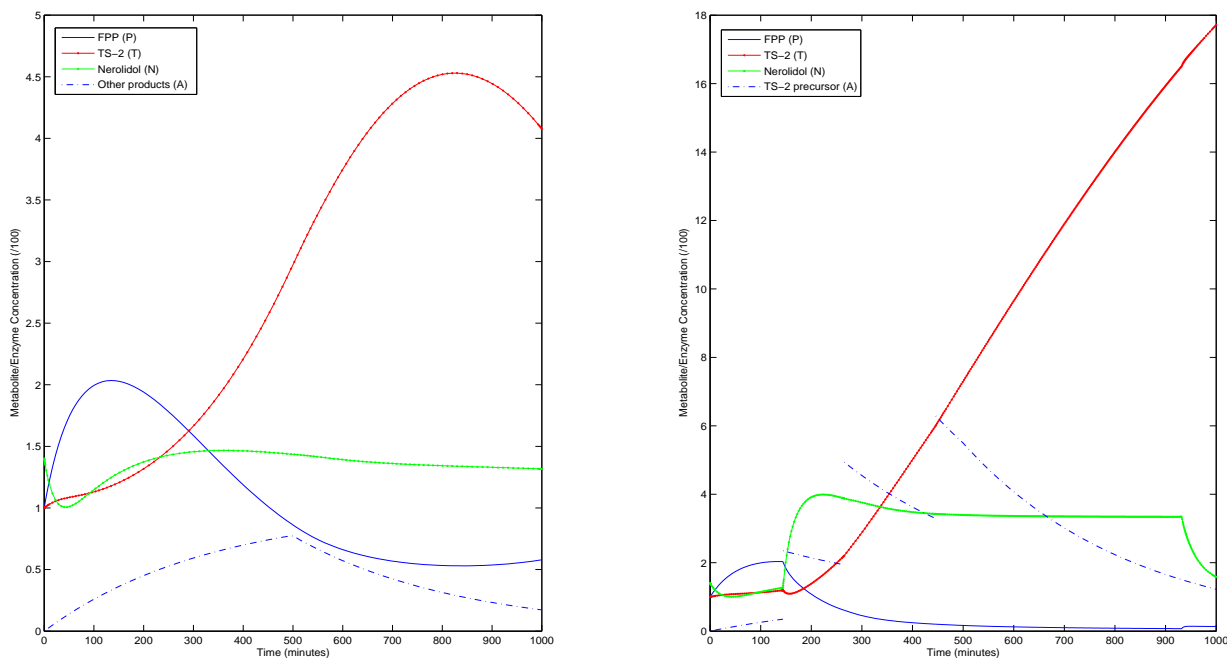


Figure 6: The change in nerolidol and enzyme (T) concentration as predicted by Model 2. The figure on the **left** is for the case of withering only (i.e. *Assamica*), whilst that on the **right** includes the effect of withering and tumbling (i.e. *Sinensis*). Note the increase in enzyme T and nerolidol concentration when tumbling is included in comparison to the right-panel of Figure 5.

During the course of the Study Group, work was also undertaken to consider the effect of a nerolidol positive-feedback loop (results not shown), that is, an increase in nerolidol leads to a subsequent increase in T , which then leads to an increase in nerolidol. However, this positive-feedback did not have any effect on the concentration of nerolidol due to the process being limited by the amount of precursor FPP (P) available. These results are far from conclusive and further information on the respective concentration of P is required before any further conclusions can be drawn.

2.4 Model 3 - Up-regulating nerolidol *via* P and T

¹We leave the equation for the activator unchanged (equation (13)), but the upregulation term at the end of equation (15) is now added to the equation for $P = \text{FPP}$ to (14).

$$\frac{dA}{dt} = k_5 H(\tau - t) - \lambda A + \sum_{j=1}^3 \gamma_j \delta(t - t_j), \quad (19)$$

¹This generalisation of the model was proposed and analysed after the study group, following a meeting of CH, AM, MT, JADW on 16/1/08.

$$\frac{dP}{dt} = \alpha_P - k_2PT - \frac{k_3PTA^q}{A_c^q + A^q} + \frac{k_6A^q}{K^q + A^q}, \quad (20)$$

$$\frac{dT}{dt} = \alpha_T - k_2PT - \frac{k_3PTA^q}{A_c^q + A^q} + \frac{k_4A^q}{K^q + A^q}, \quad (21)$$

$$\frac{dN}{dt} = k_2PT + \frac{mk_3PTA^q}{A_c^q + A^q} - \beta N^{2/3}, \quad (22)$$

The other changes we make are to the evaporation term, since we assume that only nerolidol close to the edges of leaves/cells can evaporate, so at larger concentrations, this should scale with $N^{2/3}$ rather than N^1 . We also replace the k_3 -upregulation which is given in (14)–(17) by the Heaviside step function with a more smooth Hill function, of the form $k_3(A) = A^q/(A_c^q + A^q)$.

The parameter values used are:

$$\begin{aligned} k_1 = \frac{1}{60}, \quad k_{-1} = \frac{1}{60} \times 10^{-3}, \quad k_2 = \frac{1}{60}, \quad k_3 = 0.2, \quad k_4 = \frac{1}{21}, \quad k_5 = 0.003, \quad k_6 = 0.8k_4, \\ K = 2.4, \quad q = 3, \quad m = 3, \quad \alpha_T = 0.03, \quad \alpha_P = 0.03, \\ \beta = 0.01, \quad \lambda = 0.003, \quad \tau = 500, \quad P_0 = 1, \quad T_0 = 1, \quad N_0 = 1.4, \quad A_c = 10. \\ t_1 = 144, \quad t_2 = 265, \quad t_3 = 446, \quad \gamma_1 = 5, \quad \gamma_2 = 15, \quad \gamma_3 = 15. \end{aligned} \quad (23)$$

The larger values for the Hill coefficients q mean that the function more closely approximates the heaviside step function, though retains the smoothness. The background production rates of P and T have been made the same, so that the background reaction $P + T \rightarrow N$ occurs without unused P or T building up. The levels of A at which the gene is upregulated, namely K and A_c have been increased, so that the first tumble increases the production of P and T but does not upregulate N production; that is, reaction (11) occurs with larger values of P and T , but not (12). Only when A exceeds a second, higher, threshold after the second tumble, does (12) become operative.

Figure 7 shows that *Sinensis* experiences an increased response in the activator due to tumbling, whereas tumbling is assumed to have no effect in *Assamica*. The increased activator levels in *Sinensis* causes increased production of both the precursor P =FPP and the enzyme T , and hence nerolidol too. The relative increases of nerolidol and enzyme for the two tea species are compared in Figure 8. The effects of the first two tumbles are clear in both panels, although the extra enzyme produced as a result of the first tumble is almost entirely used up by the time of the second tumble.

3 Conclusions

Analysis of data on the isoprenoid biosynthesis pathway for two tea species (*Assamica* and *Sinensis*) in the context of the tea-making process employed by Unilever, has allowed us to produce a simple mathematical model examining the relationship between certain metabolites and genes expressed in the pathway. Results of the data and mathematical model analysis have led us to the following conclusions:

- withering causes a stress response resulting in increased expression of the gene *TS-2* in both tea varieties;
- there is a strong correlation between tumbling and an increase in the gene expression (*TS-2*) in *Sinensis*, but not in *Assamica*. Increases in *TS-2* expression (that is, increased production of the enzyme T) produce more nerolidol (the aromatic ingredient);

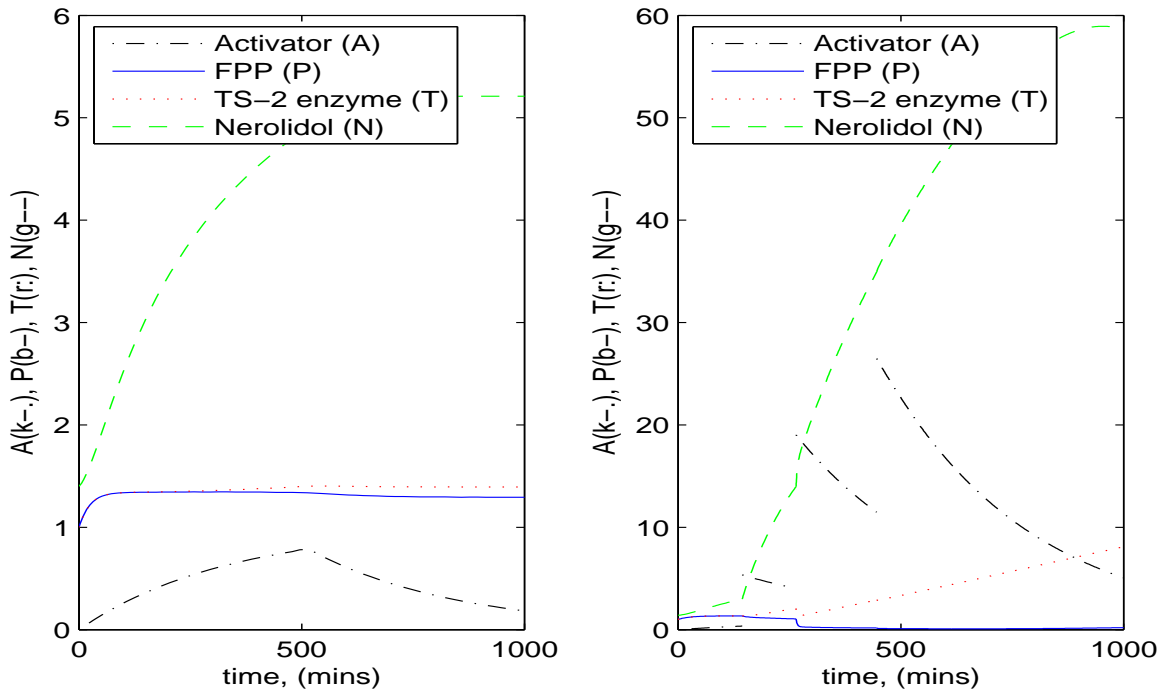


Figure 7: The changes in Activator A , FPP= P , enzyme T and Nerolidol over time for *Assamica* (left) and *Sinensis* (right) as predicted by Model 3.

- our initial simple kinetic model explains the wither response by which the gene $TS-2$ produces the enzyme T which in turn causes the production of nerolidol, but the model does not account for the tumbling response of nerolidol in *Sinensis*; and
- allowing for more nerolidol to be created through a second mechanism ((12), in addition to (11)), gives better agreement with experimental data. This mechanism provides an increased production of the enzyme T from the $TS-2$ gene when the activator A exceeds a critical level. This could be due to a simple increase in the output or efficiency of the existing pathway (11) at higher levels of A , or could be caused by the activation of a second, independent pathway.

It is important to note that our model is based on an important assumption. This assumption is that tumbling only causes a significant increase in nerolidol concentration in the case of *Sinensis* which has been subject to both tumbling and withering. We have assumed that in all other cases, that is, *Assamica* with withering only, *Assamica* with withering and tumbling and *Sinensis* with withering only, that there is no significant differences in nerolidol production.

Our work here has shown that it is the interaction between FPP, and the production of the enzyme T as a result of increased expression of the gene $TS-2$; this results in increased levels of nerolidol that is particularly important in affecting the aromatic flavour of the tea produced. Further understanding of this part of the isoprenoidal biosynthesis pathway in the context of the tea-making process is crucial. Other recommendations follow below.

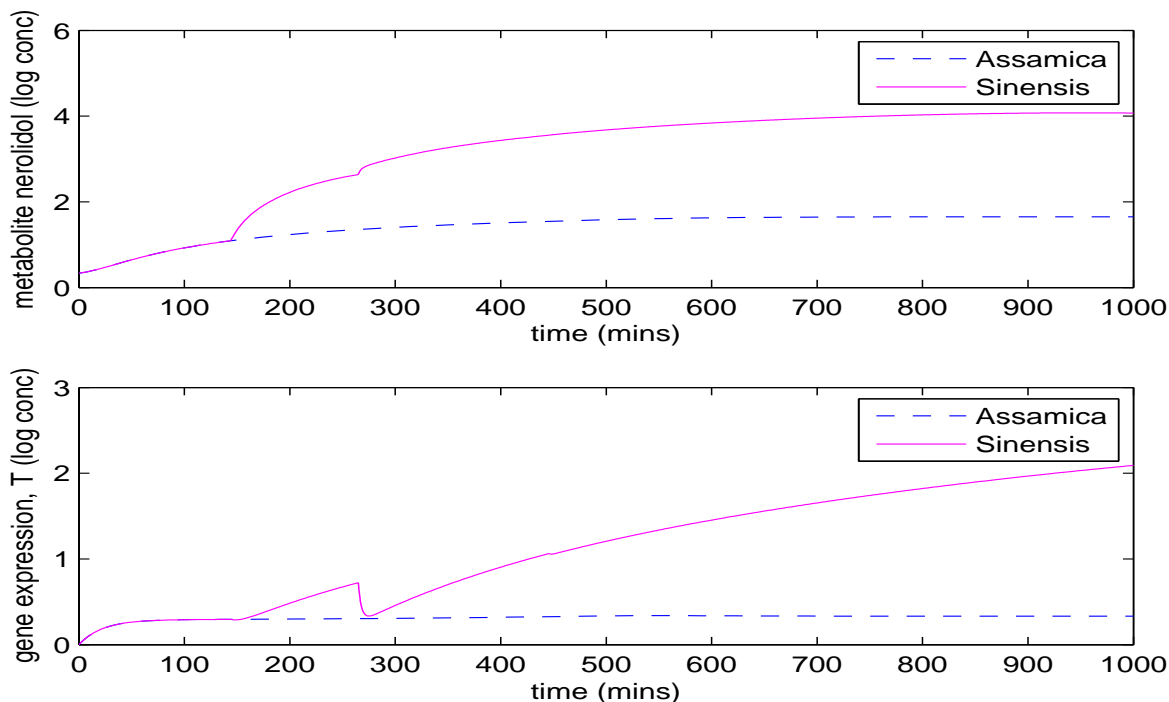


Figure 8: The change in nerolidol (**upper**) and enzyme (T , **lower**) concentration as predicted by Model 3. The solid magenta line corresponds to *Sinensis* which we assume responds to both withering and tumbling, whilst the dashed blue curve withering only (i.e. *Assamica*), which we assume only responds to withering. This figure should be compared with Figure 3.

3.1 Recommendations

The results of the work presented here suggest the following is required in order to understand the interaction between the tea-making process and the function of the metabolite pathway.

- We suggest that controlled experiments on each process separately (e.g. withering or tumbling) would provide useful control data.
- Further detail of the biochemistry of the FPP, $TS-2$, and nerolidol interaction would lead to better predictions on how nerolidol concentration is affected by the tea-making process. For example, neither of the models so far considered have a feedback mechanism by which the evaporated nerolidol (βN) can stimulate further release of nerolidol either directly or through increased production of FPP (P) or the enzyme T .
- Data on the changes in the concentration of FPP over time, either for the above-mentioned control cases or for the complete tea-making process would be useful in populating the mathematical models developed here and others in the future.

References

- [1] U ALon. An Introduction to Systems Biology: Design Principles of Biological Circuits: 10 (Mathematical & Computational Biology). Chapman & Hall/CRC, London, (2006).
- [2] E Kreyszig. Advanced Engineering Mathematics. J Wiley, New York, (1993).
- [3] JD Murray. Mathemetical Biology. Springer, Berlin, (1989).
- [4] SK Scott. Chemical Chaos, Clarendon Press, Oxford, (1991).